

DESIGN OF PMBLDC MOTOR FOR HIGH-SPEED ELECTRICAL APPLICATION

Abstract

The use of renewable energy sources as the primary source has been made possible by recent advancements on a worldwide scale. There are many other renewable energy options, but the photovoltaic system seems to have the most promise. Due to its environmental friendliness, this is the case. The PV fed Permanent Synchronous Brushless DC motor (PMBLDC) for highspeed application is presented in this system. However, PV is beneficial for wide range of applications, the output obtained from PV is low due to varying climatic factors. For increasing the voltage to a higher range, it is necessary to utilise a DC-DC converter. In this study, the enhanced CUK converter is combined with an ANFIS controller to produce stable output voltage to power the motor. The stabilized output voltage is subsequently delivered to 3ϕ VSI, which is in charge of directly powering the PMBLDC motor. Furthermore, perfect control of the inverter's frequency and voltage allows for accurate PMBLDC motor speed regulation, which is performed by comparing the reference speed with the actual motor speed using a PI controller. In addition to this, the LC filter is positioned within the PV and the inverter that assist to reduce the current and voltage fluctuation and consequently, the input feed to the inverter is smoothed. The results of a detailed simulation of the suggested technique using MATLAB reveal remarkable reliability and robustness, demonstrating the effectiveness and practicality for PV supplied PMBLDC motor drive.

Keywords: Permanent Synchronous Brushless DC Motor (PMBLDC), Improved Cuk Converter, Adaptive Network based Fuzzy Inference System controller (ANFIS), Threephase Voltage Source Inverter (3ϕ VSI).

Authors

R. Tharwin Kumar

Research Scholar
Department of Electrical and Electronics Engineering
Puducherry Technological University (Erstwhile Pondicherry Engineering College), Puducherry,
tharwin.eee@gmail.com

Riyaz A Rahiman

Associate Professor
School of Electronics and Communication,
Reva University, Bangalore, India.
riyaz.arahiman@reva.edu.in

E. Immanuelbright

Assistant Professor
Department of Department of Electrical and Electronics Engineering,
Erode Sengunthar Engineering College,
Perundurai, Erode,
immanuelbright@gmail.com

K. S. Kavim

Research Scholar
Department of Electrical and Electronics Engineering,
Government College of Engineering Tirunelveli, Tamilnadu, India.
kavinksk@gmail.com

I. INTRODUCTION

Due to the fastest growing technological development, high-speed electrical drives are widely being used. Recently, numerous manufacturing businesses as well as in devices producing electrical energy have relied on high speed motors to enable reliable and cost effective solution. For this, a variety of electric motors have been created, including stepper motors, switching reluctance motors, and permanent magnet motors (PM). In many applications, brushed motors are being replaced with electronically commutated motors (ECMs), sometimes referred to as brushless motors [1] as a result of technological advancements in motors, controllers, and feedback systems. The ECM has some advantages over brushed motors, including less environmental impact, electromagnetic radiation, and maintenance requirements. The high speed motors that are currently most in demand are electromagnetic synchronous motors, induction motors, permanent magnet synchronous motors (PMSM), direct current motors, PMBLDC motors as well as hysteresis motors [2]. These are made for lower high speed motor speed ranges, and the majority of them are not appropriate for applications requiring speeds more than 20,000 rpm. Only the PMBLDC and PMSM motors are capable of reaching speeds in the midrange and upper ranges. PMBLDC motors have a simpler design and simpler control circuitry than PMSM [3].

The beneficial properties have enabled the use of PMBLDC motors in high speed applications powered by PV arrays. Humankind is currently confronted with widespread environmental challenges including climate change and acid rain, and the creation of cleaner types of energy holds an essential to their resolution. In order to address major environmental issues, PV array, which transform solar insolation into DC electrical power, are highly helpful. However, the efficiency of the PV system is affected by weather conditions such as uniform and partial shading. As a result, it poses low voltage output. Hence power converters are required to enhance demand consumption. Several prevalent DC-DC converters were used in the traditional approaches. The most common DC-DC converter is the boost converter [4] that delivers high output voltage with low duty cycle but it causes voltage stress on the switches. Hence, a buck boost is employed which has a negative output voltage and can step down and step up. The fundamental disadvantage of buck boost converters is the discontinuous input current, which results in reduced utilisation of the input source [5]. To address the drawbacks of the buckboost converter, the derived converters CUK, SEPIC, and Zeta are introduced by combining standard buck, boost, and buck boost converters. The CUK converter's output voltage is negative and its input and output currents [6] are both constant. These converters have a low voltage conversion ratio. Therefore, the properties of boost and CUK converter are combined to form the improved CUK converter. The improved CUK converter structure offers an inverting voltage with a high voltage conversion ratio in contrast to typical DC-DC converters.

For the regulation of the output voltage constant, different control algorithms are employed in the conventional approaches. Researchers employed intelligent methods such as FLC (Fuzzy Logic Control), ANN (Artificial Neural Networks), and others. In order to combine the benefits of Fuzzy Logic and Neural network techniques, these both were integrated in a single bloc known as ANFIS, which provides superior efficiency with preferred accuracy and speed. The fuzzy system requires language rules rather than acquiring examples as prior knowledge. In addition, the input and output variables must be linguistically characterised. If the knowledge is partial, incorrect, or contradicting, the fuzzy

system must be tweaked. Because there is no formal approach, tweaking is done heuristically. This is frequently time consuming and error prone. Fuzzy systems should ideally include a neural network like [7, 8] automated adaptation process. Combining both approaches should bring together advantages while excluding negatives.

In brief, the improved Cuk converter integrated with ANFIS controller offer an excellent solution for PV-fed PMBLDC motors. The converter and related control system overcome the drawbacks of conventional methods by producing output voltage that is steady and with fewer input/output current ripples. The ANFIS controller's enhanced system reactivity and stability guarantee top notch control performance. Due to these beneficial features, the PV fed PMBLDC motor is appropriate for high power applications.

II. RELATED WORKS

Qinghu et al [9] introduces a revolutionary CWBLDC (circular winding brushless DC) motor with extreme torque density similar to BLDC motors and reduced torque ripple similar to Permanent Magnet Synchronous Motor (PMSM). Applications requiring high power and high performance can benefit from the recommended machine's circularly connected windings and commutation mechanism. The control of a CWBLDC motor, on the other hand, is reliant on an accurate rotor location. This limits those application in certain situations in which installing position sensors are challenging, and its susceptibility to electromagnetic interference may impair signal measurement in the motor and cause failure.

Wenshuo et al [10] shows a special position sensorless control method for high speed BLDC motors with low inductance and undesirable back EMF. In this work, transformational line voltages and hysteresis comparators have been used for attaining high accuracy commutation in both the moderate and extreme speed ranges. In the meantime, LPFs and transformational line voltages have been used for accomplishing maximum reliability commuter traffic in the slow zone. However, it poses some issues considering BLDC motors, connections and operation are more complicated as it involves a feedback loop and also it necessitates the use of an electronic switching controller to switch the voltage to the motor coils.

Anjaneet et al [11] shows how to develop and put into practise a dual supply buck boost converter based pump that is powered by a photovoltaic (PV) array fed switching reluctance motor (SRM). The main advantage of this DC-DC converter is that it simplifies the fabrication of gate drives by removing the requirement for switch synchronisation and connecting the regulation point to ground. But under severe loads, it experiences issues such as high inductor current and output voltage ripple.

Loic et al [12] proposed a photovoltaic transistor powered switch reluctance motor drive. The switching reluctance has various advantages, including simple and sturdy construction, produced torque in the phase winding that is unaffected by the direction of the current, as well as power from the phase winding that is returned towards the supply via feedback diodes during the off period. Even while it has many advantages, it has certain drawbacks. For high speed operations, the created torque has undesired ripples. As a result, unpleasant noises (or) acoustic losses emerge.

Anshul et al [13] discusses a three phase reluctance synchronous motor (RSM) driven intelligent grid integrated solar photovoltaic (PV) powered water pumping system. Reluctance Synchronous motors are ideal for a variety of applications because it generates extraordinarily high power density at a lower cost. Additionally, the RSM drive's speed sensorless operation boosts robustness and dependability. However, the main drawbacks include strong torque ripple when used at lower speeds, which also produces noise, the need for speed synchronisation to inverter output frequency via rotor position sensor and sensorless control, as well as the fact that the RSM drive is a little bit heavier and has a lower power factor.

III. PROPOSED TOPOLOGY AND ITS OPERATIONS

1. Description of the Proposed System: Figure 1 depicts the PMBLDC electric motor driven by solar PV array. The PV array is utilised to power the PMBLDC motor. The usage of a DC-DC converter is required to get the most out of a solar PV array because the electricity supplied by solar panels is affected by a number of elements due to the rapidly changing climatic circumstances and thus provides a low output. In this topology, a Cuk converter and the ANFIS controller are employed. The controller tunes the PI parameters to increase the performance of the improved Cuk converter. It adjusts the control parameters (K_p and K_i) by comparing the required reference voltage to the actual output voltage of the improved Cuk converter, allowing for more accurate and efficient system control.

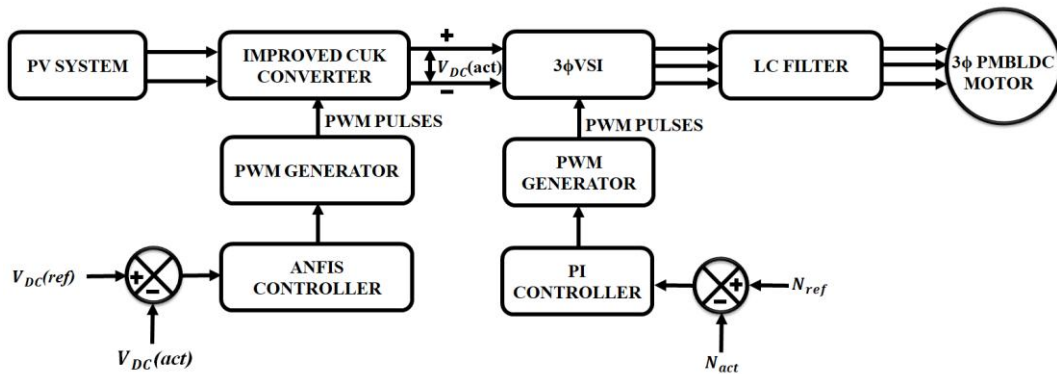


Figure 1: Schematic diagram of proposed system

By receiving an output from the controller, the PWM generator provides gating pulses to regulate the improved cuk converter. After that, the 3ϕ voltage source Inverter receives the desired output, which is in charge of directly powering the PMBLDC motor. The PMBLDC motor's speed is regulated by comparing the actual speed to the reference speed using a PI controller, which offers accurate control to the motor.

2. PV Array: PV arrays consist of PV modules connected in parallel and series. The output current and voltage have an exponential and non-linear relationship according to the solar power module specifications. The equation for a PV module's output current is provided by,

$$I_o = n_p - I_{ph} - n_p I_{rs} \exp K_o \frac{v}{n_s} - 1 \quad (1)$$

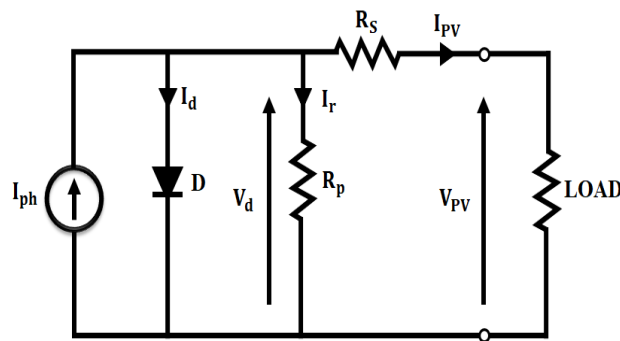


Figure 2: Equivalent circuit diagram of PV

where I_o , v represents output current and output voltage of PV respectively. Photocurrent in a cell that is corresponding to sun irradiation is denoted as I_{ph} , temperature dependent reverse saturation current of the cell is I_{rs} , K_o denotes the constant, n_p, n_s is the number of PV cells linked in parallel and series, respectively.

3. Improved Cuk Converter

Boost and buck converters fundamentally produce a Cuk converter as a cascaded consequence. This work has presented a simple switching dual structure for increasing the voltage. The step-up is composed of a pair of capacitors and a pair of diodes. To provide a novel topology known as Modified Cuk Converter (Boost Mode), the step-up structure is added to a traditional cuk converter. The suggested enhanced cuk converter's circuit architecture is shown in Fig. 3 and it operates in boost mode. This converter works in a step-up mode when the capacitor C2 and diode D2 are inserted as indicated below.

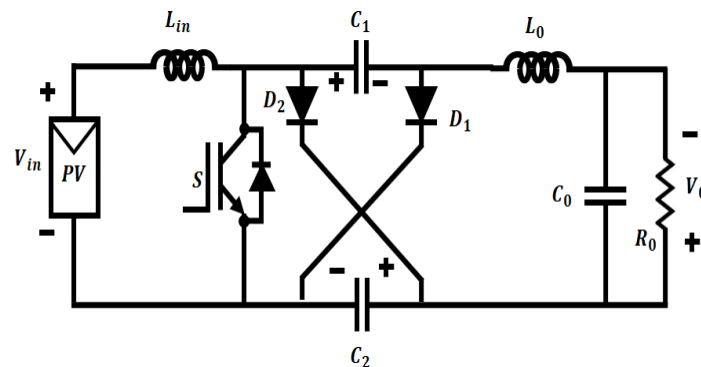


Figure 3: Circuit of Improved Cuk converter

Switching topologies of converter (T_{on} and T_{off}) mode:

Mode 1 (T_{on})

When the switch is turned ON, Capacitors C1 and C2 are discharged in series when L_{in} charges up. The relationship determines the current flowing through the switch and its associated capacitors C_1 and C_2 .

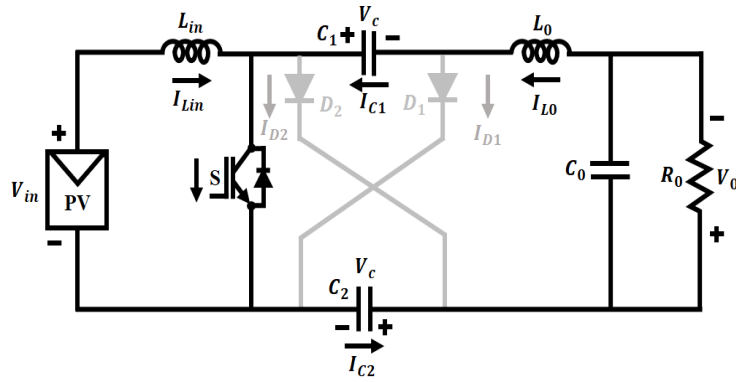


Figure 4: Circuit diagram of mode 1

$$i_{switch} = i_{in} + i_o \quad (2)$$

$$i_{c1} = i_{c2} = i_o \quad (3)$$

Mode 2 (T_{off})

Capacitors C1 and C2 are parallel charged and L_{in} is discharged once the "S" switch is toggled off. The current equations is as below:

$$i_{c1} = \frac{1}{2}(i_{in} - i_o) \quad (4)$$

$$i_{c2} = i_{c1} \quad (5)$$

$$i_{D1} = \frac{1}{2}(i_{in} + i_o) \quad (6)$$

$$i_{D2} = i_{D1} \quad (7)$$

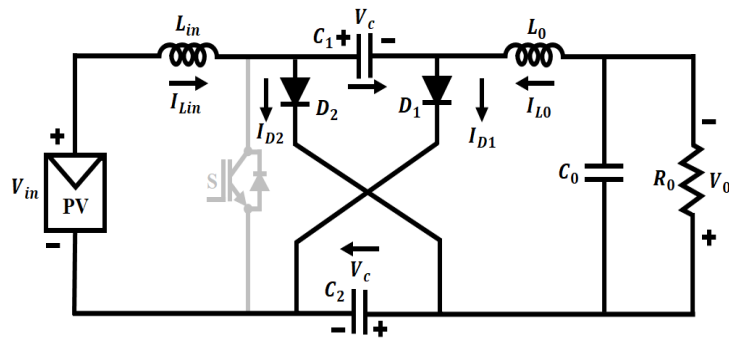


Figure 5: Circuit diagram of mode 2

The voltage balances on L_{in} and L_{out} are provided by,

$$V_{in}D + (V_{in} - V_c)(1 - D) = 0 \quad (8)$$

$$V_o - 2V_cD + (V_o - V_c)(1 - D) = 0 \quad (9)$$

So, the output voltage is expressed as,

$$V_o = \frac{1+D}{1-D} V_{in} \quad (10)$$

The drive circuit is made easier by a switch in the shunt connection. The stress on the switch, diode, and capacitor (C1) is reduced by the addition of capacitor (C2) in the proposed improved cuk converter. As a result, the PV system provides the higher efficiency with the least amount of complexity.

4. ANFIS Controller

A neural network and a fuzzy system are combined to create an adaptive network based fuzzy inference system, commonly referred to as a neuro fuzzy approach. This hybrid model will initially model the output data using the fuzzy model's variables and rules as input. The fuzzy rules are subsequently adjusted by the neural network.

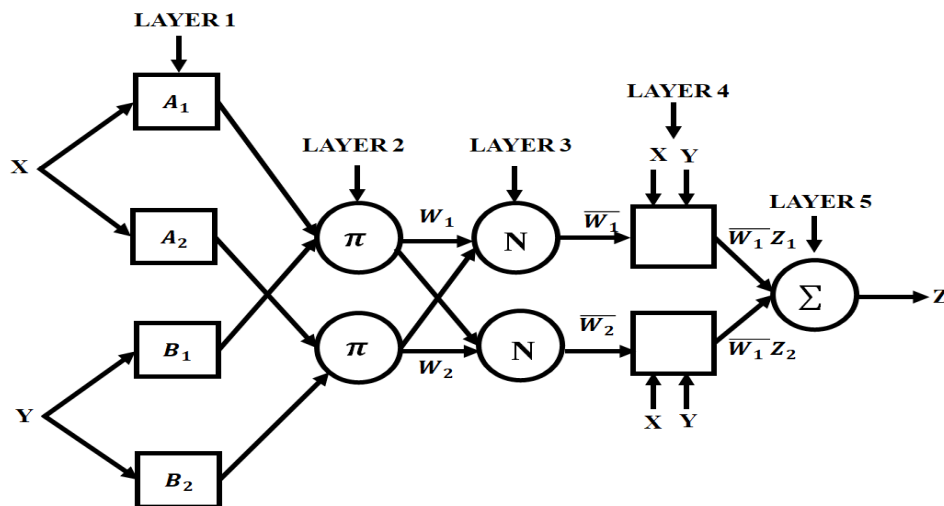


Figure 6: Typical structure of ANFIS

In ANFIS, (x, y) are taken as inputs and Z as the output which involves five layers. In the initial layer, the nodes (A_1, B_1) has the membership function assigned to each input (x, y) and at the next layer it includes two rules such as rule 1: $X = A_2$ and $y = B_1$; rule 2: $X = A_2$ and $Y = B_2$. At the third layer, the normalized firing strength is computed for every (w_1, w_2) and then the linear functions are present in the fourth layer which is the input signal function. Each rule comprises the normalized firing strength that is evaluated at the precedent layer. Finally, the overall performance is computed at the fifth layer which sums up all the incoming signals. The membership function's parameters are tuned using the trained data. In this work, to regularize the output power to load in improved CUK converter, an ANFIS based control system is employed which is demonstrated in figure7.

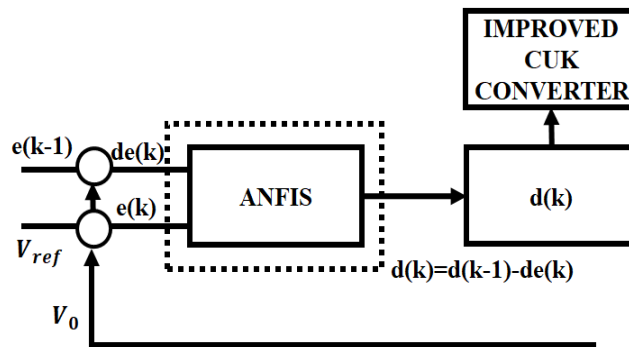


Figure 7: ANFIS control system

The ANFIS controller suggested in this study takes into account X and Y , which are error and change in error, respectively, as input parameters and Z , which is duty cycle change, as the output parameter. The duty cycle $z(k)$, in the k th sampling period, is created by adding the duty cycle $[z(k-1)]$ and the expected variance in duty cycle Z .

$$Z(k) = Z(k - 1) + Z \quad (11)$$

The immediate RMS measurements of the sine reference and load voltage are used to calculate the error X and change in error Y signals at each sample interval. These X and Y signals are then used as the input to the ANFIS controller.

$$X = V_r - V_L \quad (12)$$

$$Y = X - PX \quad (13)$$

Where, V_r and V_L denotes the reference and actual output voltages. The ANFIS controller decides what the converter's duty ratio should be. If the output voltage increases linearly with less current during charging, the ANFIS controller will maintain the voltage increase until the required point is reached.

5. Modelling of PMBLDC Motor

The usage of PMBLDC motors in power intensive system is widespread as it uses electronic commutators in place of brushes that are used in other motors and it poses best features compared to other prevalent motors such as taking up less space, not requiring external excitation, being less expensive and improved speed torque characteristics.

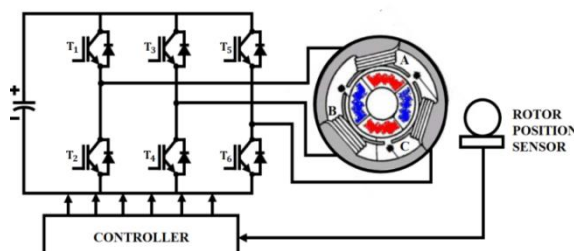


Figure 8: Circuit of PMBLDC motor

The mathematical expression of the phase voltage equations for a PMBLDC motor are as follows,

$$V_a = R_a I_a + L \left(\frac{dI_a}{dt} \right) + E_a \quad (14)$$

$$V_b = R_b I_b + L \left(\frac{dI_b}{dt} \right) + E_b \quad (15)$$

$$V_c = R_c I_c + L \left(\frac{dI_c}{dt} \right) + E_c \quad (16)$$

Where the relations of back EMFs (E_a, E_b, E_c), phase voltages (V_a, V_b, V_c) and phase currents (I_a, I_b, I_c) are shown.

The expression of the back EMF'S are computed as shown below,

$$E_a = K_e \omega_m F(\theta_e) \quad (17)$$

$$E_b = K_e \omega_m F\left(\theta_e - \frac{2\pi}{3}\right) \quad (18)$$

$$E_c = K_e \omega_m F\left(\theta_e + \frac{2\pi}{3}\right) \quad (19)$$

Where ω_m represents the angular speed, θ_c is the angle of the electrical rotor and $F(\theta_c)$ indicates the back EMF reference function of rotor position.

A PI controller operates to manage the motor's pace, comparing the reference speed to the actual motor speed and delivering exact control.

IV. RESULTS AND DISCUSSION

MATLAB is used to analyse the suggested technique and run simulations. Results are generated and explained under both constant and variable operating circumstances. The PV output is sent to the improved CUK converter, which is controlled by the ANFIS controller and provides a constant output voltage, because the PV output changes with irradiance and is of a changing nature. It is not practicable to feed a load with such a variable output potential.

Table 1: Parameter specification

PV System	
Peak power	100W, 15 panels
Short circuit current	5.86A
Open circuit voltage	22.68V
Improved Cuk Converter	
L_{in}	1mH
L_o	1mH

C_1	$4.7\mu H$
C_2	$4.7\mu H$
C_o	$22\mu H$

Figures 9 and 10 display the waveforms of temperature and solar irradiation respectively. The graph demonstrates that, in order to test the system's effectiveness, the sun's intensity is abruptly raised from $800W/m^2$ to $1000W/m^2$ at 0.25s while the temperature is raised from $25^\circ C$ to $35^\circ C$.

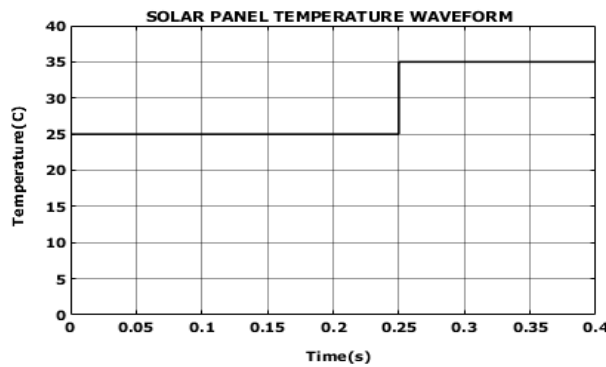


Figure 9: Waveform of solar panel temperature

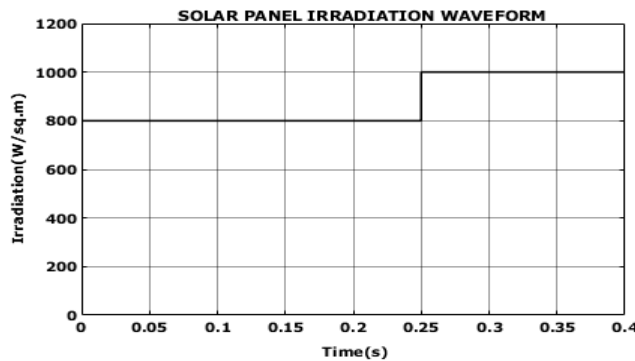


Figure 10: Solar panel irradiation waveform

The waveforms(current and voltage) of the PV system underwent significant changes as a result of the deliberate change in ambient conditions, as shown by the waveforms in Figure 11 and 12. From the figure, it is clear that the solar voltage varies from 52V to 62V and the current is maintained stable at 1A after 0.25s after a slight variation.

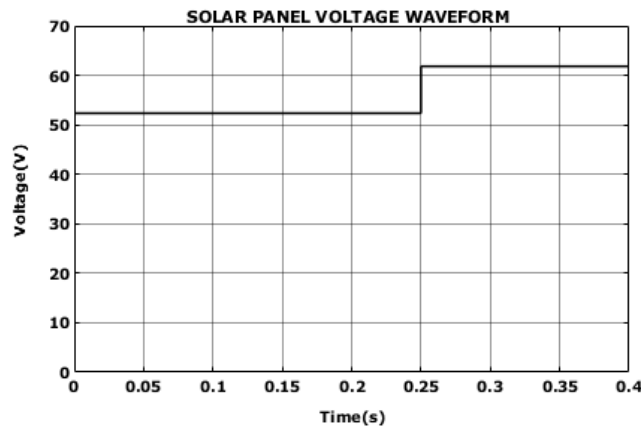


Figure 11: Voltage waveform of solar panel

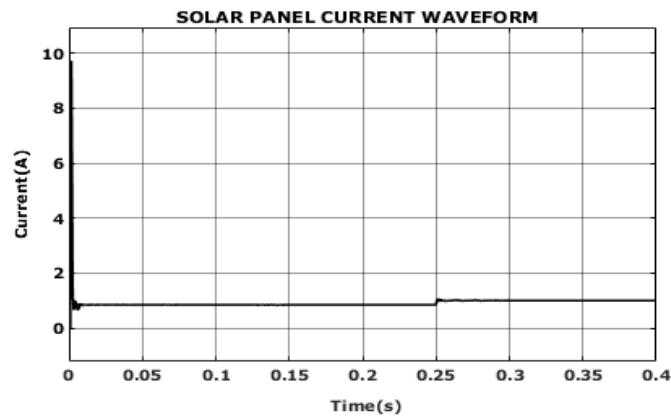


Figure 12: Current waveform of solar panel

Figures 13 and 14 illustrate the converter's voltage and current waveforms respectively. The figure clearly illustrates that the output voltage waveform outputs a constant 300V. The variation in temperature and irradiance has a direct impact on its output. As a result, the PV voltage and PV current waveforms vary in accordance with the operational state changes at 0.25s. The voltage variation in the upgraded cuk converter input, on the other hand, has no effect on its output because the converter is employed in conjunction with the ANFIS controller to provide constant output voltage.

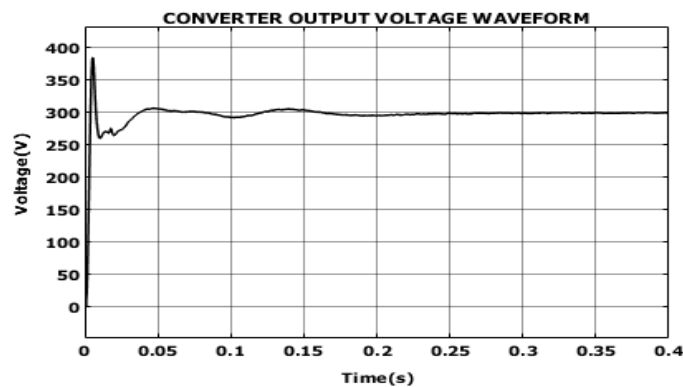


Figure 13: Output voltage waveform of converter

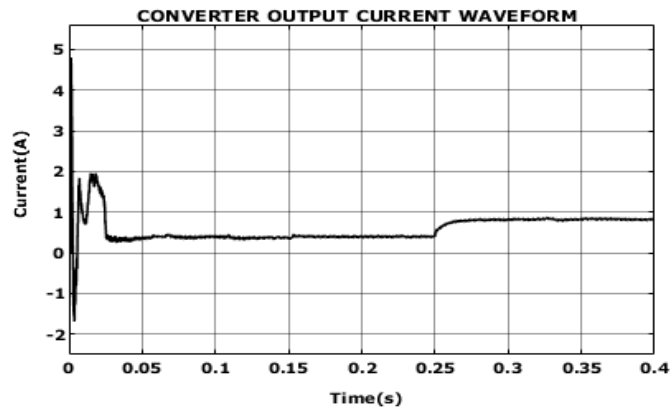


Figure 14: Output current waveform of converter

Figures 15, 16, 17, and 18 depicts the back EMF, current, torque, and speed parameters of a PMBLDC motor respectively. When comparing the PI Controller to other controllers, it can be seen from the PMBLDC motor waveform that it offers greater influence over the motor's output speed. It has also considerably lessened output torque ripples.

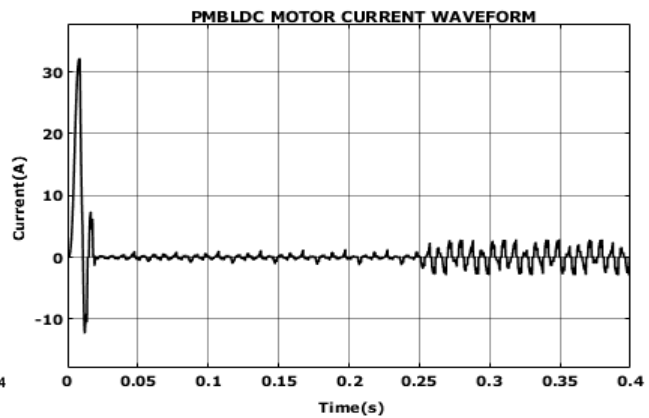
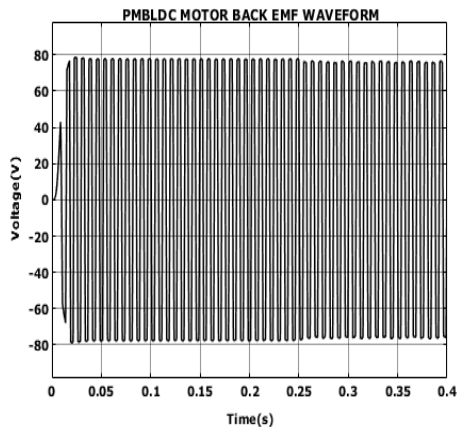


Figure 15: PMBLDC motor back EMF waveform **Figure 16:** PMBLDC motor- current waveform

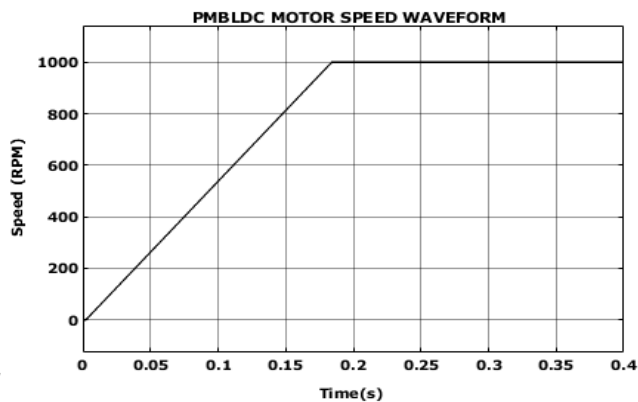
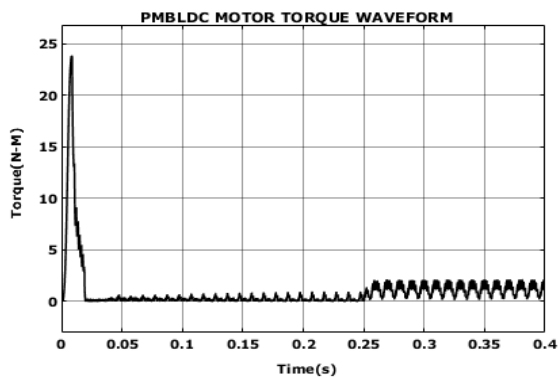


Figure 17: PMBLDC motor-Torque waveform **Figure 18:** PMBLDC motor's speed waveform

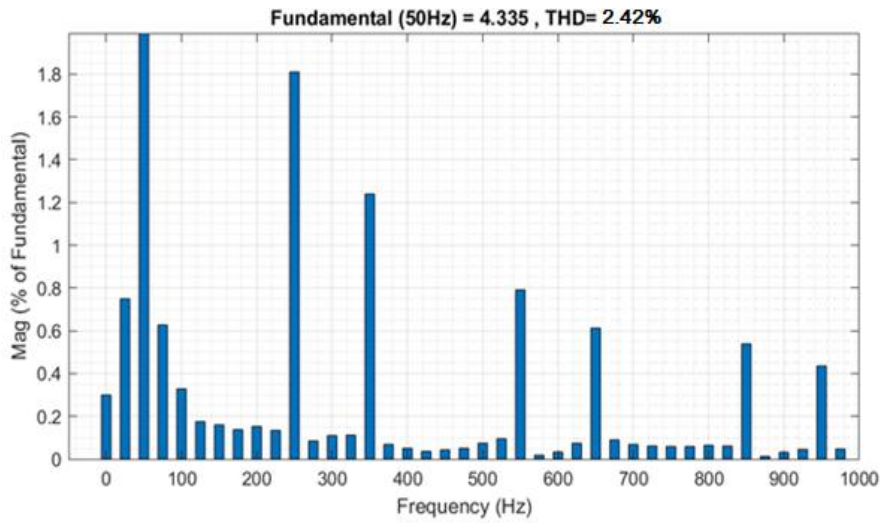


Figure 19: Total Harmonic Distortion

Figure 19 depicts the Total Harmonic Distortion. The figure clearly indicates that the improved cuk converter with ANFIS controller achieves low harmonic distortion of 2.42%, demonstrating the system's efficiency with improved power quality.

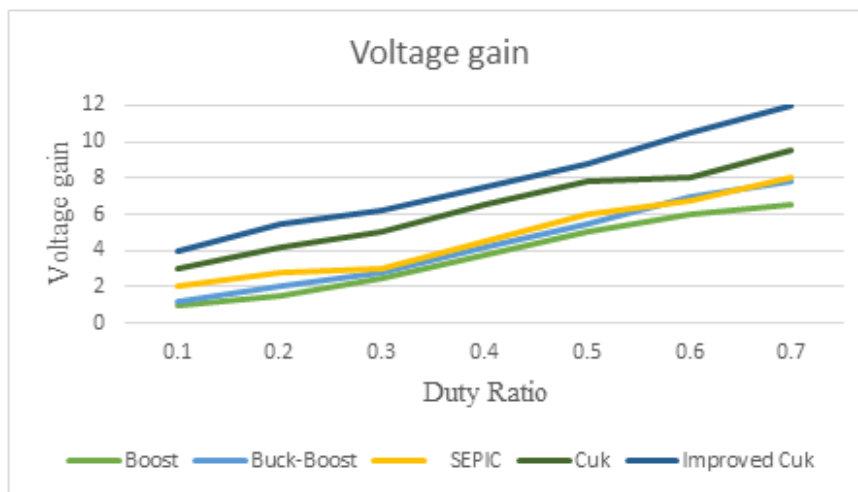


Figure 20: Comparison of Voltage gain Vs Duty Ratio

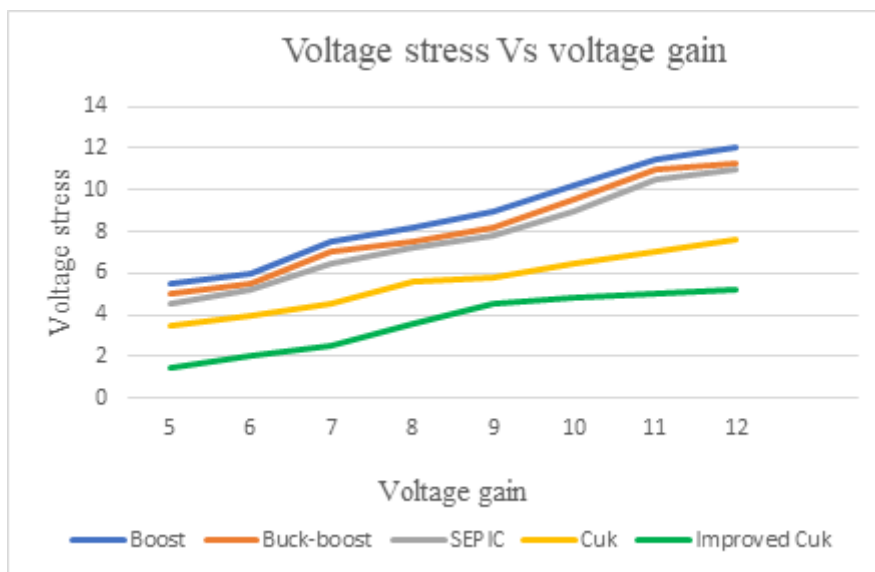


Figure 21: Comparison of Voltage stress Vs Voltage gain

From the comparison graph shown in figure 20 and 21, it is clear that the high voltage gain is achieved by improved cuk converter compared to other converters which includes boost, buck-boost, SEPIC and conventional cuk converter which is shown in figure 20. With the improved Cuk converter, the voltage stress is minimized which is shown in figure 21.

V. CONCLUSION

In this work, the PMBLDC motor powered by solar PV array utilizing improved cuk converter is presented. The improved cuk converter integrated with ANFIS controller provides efficient power delivery. The simulation's results show whether the system's performance is viable. It proves that the suggested method outperforms the other conventional technology used to drive the PMBLDC motor in a high speed application. The improved cuk converter exhibits high efficiency and it reduces the ripple current at both input and output. Furthermore, the controller improves the overall system performance by ensuring stable output. With the efficient converter and control approaches, the proposed technique achieves low harmonic distortion of 2.42%. These best features make PMBLDC motors ideal for use in high power applications, even under non-linear operating conditions.

REFERENCE

- [1] Shanming Wang, Jianfeng Hong, Yuguang Sun, Haixiang Cao 2019, "Analysis and Reduction of Electromagnetic Vibration of PM Brush DC Motors", IEEE Transactions on Industry Applications, vol. 55, no. 5, pp. 4605-4612.
- [2] Fortino Mendoza-Mondragón, Víctor Manuel Hernández-Guzmán, Juvenal Rodríguez-Reséndiz 2018, "Robust Speed Control of Permanent Magnet Synchronous Motors Using Two-Degrees-of-Freedom Control", IEEE Transactions on Industrial Electronics vol. 65, no. 5, pp. 6099-6108.
- [3] Zhi Yang, Fei Shang, Ian P. Brown, Mahesh Krishnamurthy 2015, "Comparative Study of Interior Permanent Magnet, Induction and Switched Reluctance Motor Drives for EV and HEV Applications", IEEE Transactions on Transportation Electrification, vol. 1, no. 10, pp. 245-254.
- [4] M. Arjun, Vanjari Venkata Ramana, Roopa Viswadev, B. Venkatesaperumal 2020, "Small Signal Model for PV Fed Boost Converter in Continuous and Discontinuous Conduction Modes", IEEE Transactions on Circuits and Systems II: Express Briefs, vol. 8, no. 6, pp. 1192-1196.

- [5] Balaji Chandrasekar, ChellammalNallaperumal, SanjeevikumarPadmanaban, Mahajan Sagar Bhaskar, Jens Bo Holm-Nielsen, Zbigniew Leonowicz, Samson O. Masebinu 2019, “Non-Isolated High-Gain Triple Port DC–DC Buck-Boost Converter With Positive Output Voltage for Photovoltaic Applications”, IEEE Access, vol. 66, no. 7, pp. 1192-1196.
- [6] Radha Kushwaha, Bhim Singh 2019, “A Power Quality Improved EV Charger With Bridgeless Cuk Converter”, IEEE Transactions on Industry Applications, vol.55, no.5, pp. 5190-5203.
- [7] Hany M. Hasanien, Mahmoud Matar 2019, “A Fuzzy Logic Controller for Autonomous Operation of a Voltage Source Converter-Based Distributed Generation System”, IEEE Transactions on Smart Grid, vol. 6, no. 1, pp. 158-165.
- [8] Xiao-Fang Liu, Zhi-Hui Zhan, Jun Zhang 2022, “Resource-Aware Distributed Differential Evolution for Training Expensive Neural-Network-Based Controller in Power Electronic Circuit”, IEEE Transactions on Neural Networks and Learning Systems, vol. 33, no.11, pp. 6286-6296.
- [9] Qinghu Zhang, Siwei Cheng, Dong Wang, Zhewu Jia 2018, “Multiobjective Design Optimization of High-Power Circular Winding Brushless DC Motor”, IEEE Transactions on Industrial Electronics, vol. 65, no. 2, pp. 1740-1750.
- [10] Wenzhuo Li, Jiancheng Fang, Haitao Li, Jiqiang Tang 2016, “Position Sensorless Control Without Phase Shifter for High-Speed BLDC Motors With Low Inductance and Nonideal Back EMF”, IEEE Transactions on Power Electronics, vol.31, no. 2, pp. 1354-1366.
- [11] Anjanee Kumar Mishra, Bhim Singh 2017, “Solar Photovoltaic Array Dependent Dual Output Converter Based Water Pumping Using Switched Reluctance Motor Drive”, IEEE Transactions on Industry Applications, vol. 53, no. 7, pp. 5615-5623.
- [12] LoïcQuéval, Alain Coty, Lionel Vido, RaimundGottkehaskamp, Bernard Multon 2017, “A Switched Reluctance Motor Drive Using Photovoltaic Transistors: Principle, Prototype, Experimental, and Numerical Results”, IEEE Transactions on Industry Applications, vol. 53, n0. 5, pp. 4886-4893.
- [13] Anshul Varshney, Utkarsh Sharma, Bhim Singh 2021, “An Intelligent Grid Integrated Solar PV Array Fed RSM Drive-Based Water Pumping System”, IEEE Transactions on Industry Applications, vol. 57, no. 2, pp.1818-1829.